Supplementary information for "*Ferroelectric control of diverse hyperbolic polaritons in the visible spectrum*"

Zailong Chen[1], Shengxuan Xia[2,‡], Shuo Yang[1], Baomin Wang[3], Shiwei Tang[3], Yurong Yang[4], Tian Cui[1], Shi Liu[5,§], Hongwei Wang[1,*]

[1]*Institute of High-Pressure Physics, School of Physical Science and Technology, Ningbo University, Ningbo 315211, China*

[2] *School of Physics and Electronics, Hunan University, Changsha 410082, China*

[3] *School of Physical Science and Technology, Ningbo University, Ningbo 315211, China*

[4]*Laboratory of Solid-State Microstructures, Jiangsu Key Laboratory of Artificial Functional Materials, Nanjing University. Nanjing 210093, China*

[5] *Department of Physics, School of Science, Westlake University, Hangzhou, Zhejiang 310030, China*

Corresponding Authors: *wanghongwei@nbu.edu.cn; §liushi@westlake.edu.cn; ‡shengxuanxia@hnu.edu.cn

Supplementary Notes

1. The optical absorption in bulk $WOBr_4$ perpendicular to the chain direction

In the main text, we have elaborately elucidated the physical nature for optical absorption in bulk $WOBr_4$ along the chain direction, which exhibits the flexible tunability to applied electric field and uniaxial strain. Here, we interpret the optical behaviors perpendicular to the chain direction that is less sensitive to the external stimuli. As shown in **Fig. S4(a)**, the primary optical absorption peak perpendicular to the chain direction is dictated by interband transitions from $V_{1\text{-}6}$ to $C_{1\text{-}2}$ bands. The $C_{1\text{-}2}$ and $V_{1\text{-}6}$ bands are composed of the $\mathbf{d_{xy}}$ orbitals of the W atom and the $\mathbf{p_x}$ and $\mathbf{p_y}$ orbitals of the Br atom (**see Fig. S4(b)**), respectively. In general, the energy levels of **d** orbitals are regulated through the crystal field generated by surrounding octahedral ligands. The relationship between energy levels of **d** orbitals and **z**-uniaxial strain is presented in **Fig. S4(c)**. The $\mathbf{d_{xz}}$, $\mathbf{d_{yz}}$ and $\mathbf{d_{z2}}$ orbitals lying out-of-plane exhibit notable energy variations with the **z**-uniaxial strain, which is attributed to modulated repulsive interplay between central W and apical O atoms, driven by the evolution of the ferroelectric mode. However, the in-plane $\mathbf{d_{x2\text{-}y2}}$ and $\mathbf{d_{xy}}$ orbitals are only minimally affected by the ferroelectric mode, due to their weak interaction with the apical O atom. As a result, the shape and symmetry of $\mathbf{d_{xy}}$ orbital exhibits a negligible variation under external stimuli (**Fig. S4(d)**), accounting for the weak tunability of optical absorption perpendicular to the chain direction.

2. Ferroelectric manipulated optical properties in 1D oxytetrahalide $WOCl_4$

We validated our proposed mechanisms for another experimentally synthesized 1D oxytetrahalide $WOCl_4$ that also presents robust ferroelectricity along the chain direction and anisotropic optical behaviors[1,2]. The absorption peaks of $WOCl_4$ exhibit certain tunability under uniaxial strain and electric field as shown in **Figs. S5(a)** and **S5(b)**, but with weaker effects in contrast to $WOBr_4$. The underlying mechanism is attributed to weakly coupled ferroelectric polarization with external strain and electric field (**see Fig. S5(c)**). When ferroelectric polarization

of $WOCl_4$ is manually reduced to zero, its absorption peak shows a significant enhancement, comparable to that of $WOBr_4$, as shown in **Fig. S5(d)**. Therefore, these phenomena in $WOCl_4$ further demonstrate that the ferroelectric order is the key factor to regulating optical behaviors in 1D oxytetrahalide materials.

Supplementary Figures

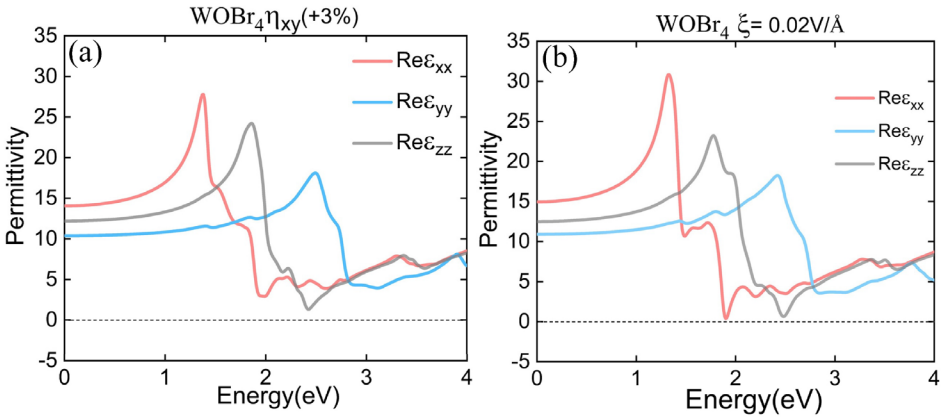

Figure S1 **Tunable optical permittivity in monolayer $WOBr_4$. (a)-(b)** Real part of optical dielectric spectra of $WOBr_4$ under **(a)** 3% **x-y**-biaxial strain and **(b)** an electric field of 0.02 V/Å.

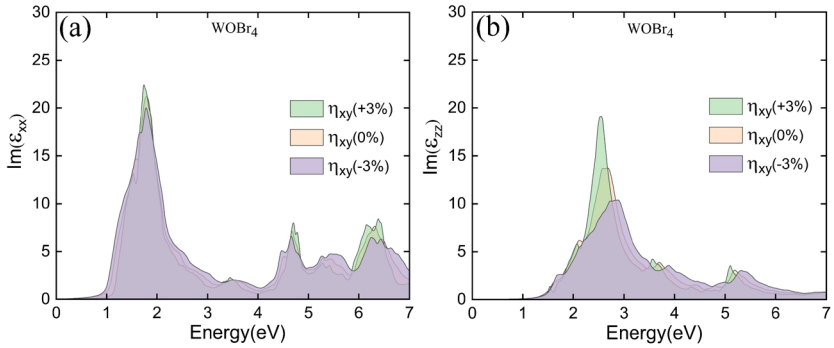

Figure S2 **Strain tunable optical dielectric spectra in bulk $WOBr_4$. (a)-(b)** Imaginary part of optical dielectric spectra of $WOBr_4$ in the **(a)** $\hat{x}$ and **(b)** $\hat{z}$ directions under 3%, 0%, and -3% **x-y**-biaxial strains.

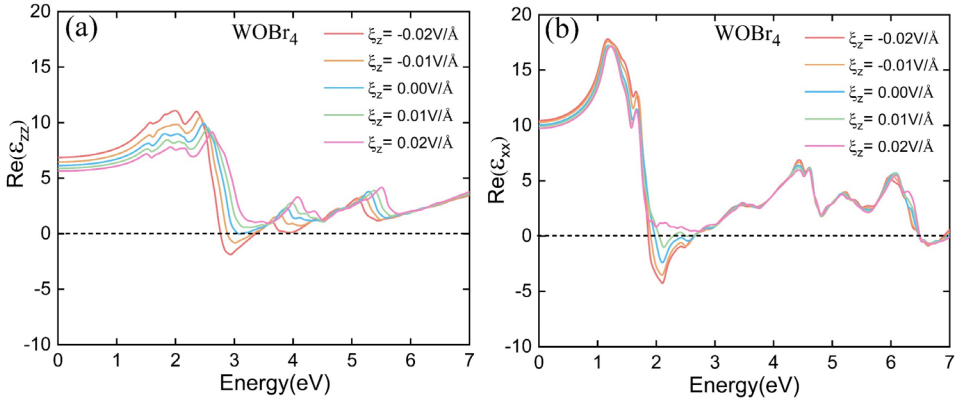

Figure S3 **Optical dielectric spectra of $WOBr_4$ under electric boundary conditions. (a)-(b)** Real part of optical dielectric spectra in the **(a)** $\hat{z}$ and **(b)** $\hat{x}$ directions under successive electric fields, ranging from -0.02 V/Å to 0.02 V/Å.

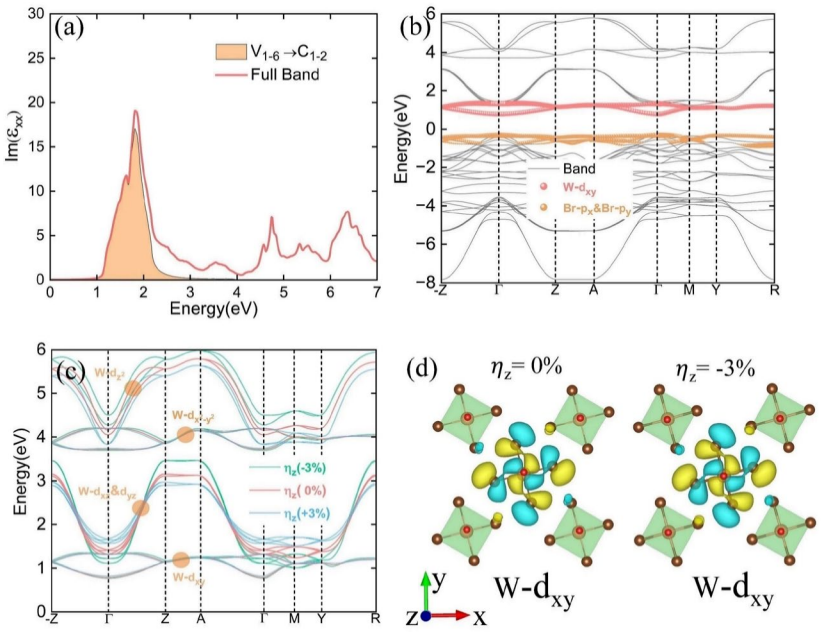

Figure S4 **Microscopic origin of low-energy optical absorption peak in $WOBr_4$. (a)** Imaginary part of optical dielectric spectrum in the $\hat{z}$ direction contributed by partial interband transitions (yellow shaded area) from 1-6 valence bands ($V_{1\text{-}6}$) to 1-2 conduction bands ($C_{1\text{-}2}$), where the band number is ordered based on their energy difference related to the Fermi level. The imaginary part of optical dielectric spectrum of full interband transition is plotted with red curve for comparison. **(b)** Orbital projected band structure for $V_{1\text{-}6}$ and $C_{1\text{-}2}$ bands that involve the interband transitions for primary absorption peak in the optical dielectric spectrum. **(c)** The variations of band structures with various **z**-uniaxial strains in relation to **d** orbitals of the W atom. **(d)** Plot of $\mathbf{d_{xy}}$ Wannier orbital for the structures under 0%, and -3% the **z**-uniaxial strains.

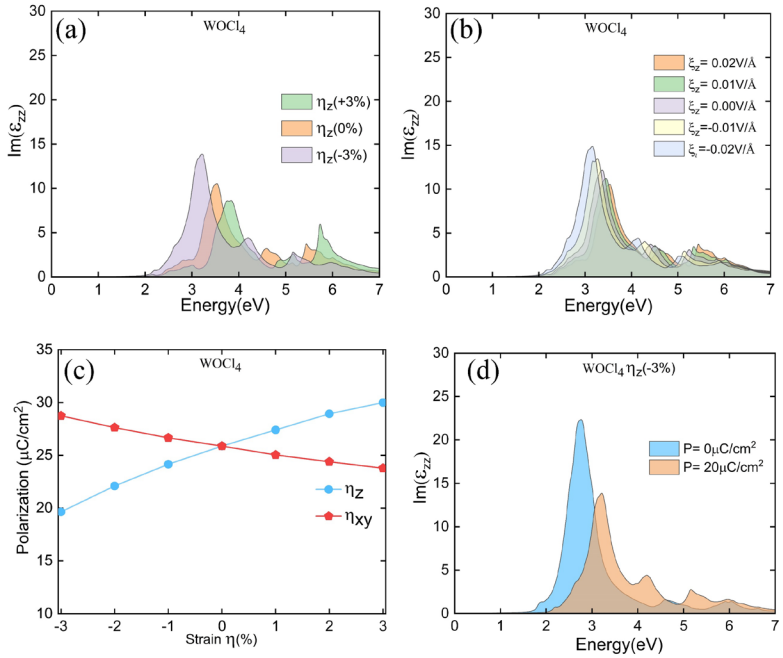

Figure S5 **Optical and ferroelectric properties of $WOCl_4$ under electric and mechanic boundary conditions. (a)** Imaginary part of optical dielectric spectra in the $\hat{z}$ direction under -3%, 0% and 3% **z**-uniaxial strains. **(b)** Imaginary part of optical dielectric spectra in the $\hat{z}$ direction under successive electric fields ranging from -0.02 V/Å to 0.02 V/Å. **(c)** Polarization of $WOCl_4$ as a function of **z**-uniaxial strain and **x-y** biaxial strain. **(d)** Imaginary part of optical dielectric spectra in the $\hat{z}$ direction for structures with ferroelectric polarizations of $20\mu C/cm^2$ and $0\mu C/cm^2$.

Supplementary Reference

1 Hess, H. & Hartung, H. Die Kristallstruktur von Wolframoxidchlorid $WOCl_4$ und Wolframoxidbromid $WOBr_4$. *Z. Anorg. Allg. Chem.* **344**, 157-166 (1966).

2 Lin, L., Zhang, Y., Moreo, A., Dagotto, E. & Dong, S. Quasi-one-dimensional ferroelectricity and piezoelectricity in WOX_4 halogens. *Phys. Rev. Mater.* **3**, 111401 (2019).